NIH Public Access
Author Manuscript
*J Am Chem Soc*. Author manuscript; available in PMC 2014 May 01.

Published in final edited form as:
*J Am Chem Soc*. 2013 May 1; 135(17): 6633–6642. doi:10.1021/ja4015937.

# Mechanism of Alkoxy Groups Substitution by Grignard Reagents on Aromatic Rings and Experimental Verification of Theoretical Predictions of Anomalous Reactions

**Gonzalo Jiménez-Osés**[†], **Anthony J. Brockway**[‡], **Jared T. Shaw**[‡,*], and **K. N. Houk**[†,*]

[†]Department of Chemistry and Biochemistry, University of California, Los Angeles, Los Angeles, California 90095-1569, United States.

[‡]Department of Chemistry, One Shields Ave, University of California, Davis, California 95616, United States.

## Abstract

The mechanism of direct displacement of alkoxy groups in vinylogous and aromatic esters by Grignard reagents, a reaction that is not observed with expectedly better tosyloxy leaving groups, is elucidated computationally. The mechanism of this reaction has been determined to proceed through the inner-sphere attack of nucleophilic alkyl groups from magnesium to the reacting carbons via a metalaoxetane transition state. The formation of a strong magnesium chelate with the reacting alkoxy and carbonyl groups dictates the observed reactivity and selectivity. The influence of ester, ketone and aldehyde substituents was investigated. In some cases, the calculations predicted the formation of products different than those previously reported; these predictions were then verified experimentally. The importance of studying the actual system, and not simplified models as computational systems, is demonstrated.

## Introduction

The substitution of alkoxy groups on aromatics ($S_NAr$) activated by *ortho*-carbonyl substitution[1] has been known for a number of early examples in the literature,[2–21] but this reaction has been shown to be quite general in recent studies by our group. A general example with 1-methoxynaphthalenes is shown in Scheme 1a. Related reactions are found in non-aromatic systems (Scheme 1b). While the reactions shown are tolerant to other alkoxy groups, the normally better leaving group tosyloxy is not displaced. In addition, while many Grignard reagents are effective, organolithium and organozinc reagents give poor yields at best. We report a computational study of this reaction that provides a thorough mechanistic rationale of these facts. Furthermore, in some cases, theory predicts the formation of different products from those originally assigned, and these predictions have been verified experimentally.

**Corresponding Author**: houk@chem.ucla.edu, jtshaw@ucdavis.edu.

**ASSOCIATED CONTENT**

**Supporting Information**. Additional figures, cartesian coordinates, electronic energies, entropies, enthalpies, Gibbs free energies, lowest frequencies of the different conformations of all structures considered. This material is available free of charge via the Internet at http://pubs.acs.org.

NIH-PA Author Manuscript
NIH-PA Author Manuscript
NIH-PA Author Manuscript

NIH-PA Author Manuscript

NIH-PA Author Manuscript

NIH-PA Author Manuscript

## Results and Discussion

### Reaction mechanism

While metallic chelates of 1,3 and 1,4-alkoxycarbonyl compounds have been detected by NMR spectroscopy[22–24] we were unable to identify these complexes in solution using magnesium halides as chelating agents, due to their insolubility in the deuterated reaction solvents. Instead, we have performed a computational study of all conceivable bidentate complexation modes of $CH_3MgCl$ to methyl 1-methoxy-2-naphthoate **1a**. Although most experiments were performed with ethyl or larger Grignards, our initial calculations involved methyl Grignard reagents for simplicity. The well-known μ-dichloro dimer form of Grignard reagent[25–28] including two solvent molecules (dimethyl ether, DME, in our model) was selected as the starting material, and several dimer and monomer isomers of the reactant complex, denoted as **1a•CH$_3$MgCl (a-m)**, were calculated. Figure 1 shows the geometries and formation energies of the most significant structures for these complexes (see Figure S1 in Supporting Information for further details). The Schlenk equilibrium [29] (*i.e.* formation of dialkyl magnesium compounds and magnesium halide salts) was not considered to take place significantly under the experimental conditions. The monomeric magnesium chelate **1a•CH$_3$MgCl (a)** formed after scission of two Mg–Cl bonds upon substrate coordination was by far the most stable complex in solution ($\Delta G_{complex}$ = −7.2 kcal mol$^{-1}$), whereas the formation of complexes with Grignard dimer species was always endergonic ($\Delta G_{complex}$ = +2.4 to +10.9 kcal mol$^{-1}$). This complex was considered the reference minimum for the estimation of the free energy barriers calculated here.

The classical mechanism of Grignard reagents addition to carbonyl compounds, especially ketones, was first proposed by Ashby.[25–28,30] This mechanism involves the participation of a μ-chloro organomagnesium dimer in which one Mg is coordinated to the carbonyl oxygen, and the other Mg delivers the alkyl or aryl nucleophile to the carbonyl carbon through a concerted six-membered cyclic transition state (TS) (Figure 2). When we calculated this mechanism starting from complex **1a•CH$_3$MgCl (d)**, it was first necessary to cleave one Mg–Cl bond and coordinate one ether molecule to provide a reasonable coordination environment for the Mg transferring the nucleophile. This rearrangement barely stabilized the new reactant complex **1a•CH$_3$MgCl(DME) (d')** by 0.4 kcal mol$^{-1}$ over the unsolvated μ-dichloro species. In the proposed six-membered TS geometry, both for the addition to the carbonyl or the alkoxy displacement, the alkyl group suffers pyramidal inversion at the reacting carbon during the C–C bond formation, at a significant energy cost. Accordingly, quite high energy barriers for the addition to *ipso* position in the naphthalene ring and 1,2-addition to the ester carbonyl were calculated ($\Delta G^{\ddagger}_{OMe}$ = +32.7 for **1a-TS'$_{OMe}$** and $\Delta G^{\ddagger}_{C=O}$ = +28.2 kcal mol$^{-1}$ for **1a-TS'$_{C=O}$**, respectively). Moreover, the favored addition to the carbonyl group by 4.5 kcal mol$^{-1}$ completely disagrees with the experimental observations.

These results prompted us to investigate alternative pathways for the studied reactions. Looking at the structure of the most stable magnesium chelate **1a•CH$_3$MgCl (a)**, in which the nucleophilic alkyl group is located proximal to both reacting carbons at the methoxy and ester groups (3.85 and 4.04 Å respectively), we envisaged a direct transfer of the methyl group to either the carbonyl or *ipso* aromatic carbons through a four-membered metalaoxetane TS (Figure 2). Despite the apparently more strained arrangement of these TS with respect to the aforementioned six-membered TS, the alkyl group is transferred from the Grignard reagent without pyramidal inversion and with minimal rehybridization of the reacting carbon. This smaller distortion of the reactants in the TS provides a significantly lower activation barrier for the both alkyl addition processes ($\Delta G^{\ddagger}_{OMe}$ = +25.2 for **1a-TS$_{OMe}$** and $\Delta G^{\ddagger}_{C=O}$ = +24.8 kcal mol$^{-1}$ for **1a-TS$_{C=O}$**, respectively). More importantly,

NIH-PA Author Manuscript

NIH-PA Author Manuscript

NIH-PA Author Manuscript

both competitive pathways get much closer to the observed preferential displacement of the methoxy group leading to compound **2a**.

In order to test the validity of our model, the reaction of ester **1a** with $CH_3MgCl$ was assayed experimentally (Scheme 2). In agreement with our calculations, this reaction yields both 1,2- and 1,4-conjugate addition products together with a small amount of hydroxylated compound **18**. The intermediate methyl ketone was not observed and tertiary alcohol **15a** was obtained as the minor reaction product. Despite the major proportion of **2a** in the reaction mixture, 2 equiv. of Grignard reagent are consumed in the two successive 1,2-additions per equiv. consumed in the 1,4-conjugate addition; this limits the proportion of tertiary alcohol in the final mixture when stoichiometric amounts of $CH_3MgCl$ are used and suggests that the 1,2-addition to the carbonyl group must be competitive with 1,4-addition'. Hence, the formation of tertiary alcohol **15a** with methyl Grignard reagents, not reported previously for methoxynaphthyl esters, was successfully predicted by our calculations and demonstrated experimentally.

The influence of the nature of the Grignard reagent on the rate-limiting step of the reaction was investigated computationally.

In good agreement with experimental results[1] (Scheme 1), the simple substitution of MeMgCl (yielding **2a**) by EtMgBr as a closer model to *n*-BuMgCl (yielding **2b**) had a quite beneficial effect on both the calculated reactivity and chemoselectivity, providing lower activation energies and shifting to a 98:2 ratio towards methoxy group displacement (lowest energy barriers: $\Delta G^{\ddagger}_{OMe}$ = +22.1 for **1a-TS$_{OMe}$** and $\Delta G^{\ddagger}_{C=O}$ = +23.7 kcal mol$^{-1}$ for **1a-TS$_{C=O}$**, respectively). We decided to use EtMgCl as a more appropriate Grignard reagent model henceforth, since the majority of experiments were conducted using primary nucleophiles such as *n*-BuMgCl and *i*-BuMgCl.

In order to determine the rate-limiting step of each competing reaction, the whole mechanisms were calculated for both processes. As depicted in Figure 3, both reactions follow stepwise mechanisms in which the initial addition to the carbonyl or alkoxy groups is clearly the rate-limiting step. This step is moderately exergonic in both cases and leads to quite stable but very reactive tetrahedral intermediates.

Such intermediates derived from 1,2- and 1,4-conjugate addition can be visualized as magnesium alkoxides and enolates, respectively. These transient species evolve through an almost barrierless second step to cleave the methoxy leaving group and recover either naphthalene aromaticity or the carbonyl $sp^2$ hybridization. The restoration of **π**-delocalization along the aromatic and carbonyl systems, and the formation of covalent Mg-alkoxy species after leaving group departure are the driving forces for such hyper fast and highly exergonic processes. Interestingly, the formation of a tetrahedral intermediate at the *ipso* carbonyl of naphthalene does not disrupt the aromaticity and **π**-conjugation with the *ortho* carbonyl group significantly, as demonstrated by the slight exergonicity of the first reaction step. As will be discussed below, this is not the case with other position isomers of this substrate.

In our previous study,[1] we reported that non-aromatic vinylogous esters such us *Z*-ethyl 3-methoxycinnamate **3** and methyl 1-methoxy-3,4-dihydro-2-naphthoate **5** (Scheme 3) readily react with Grignard reagents in a similar manner to the naphthalene counterparts, namely with complete selectivity towards alkoxy group displacement. However, treatment of the corresponding 1H-indene analogue **7** with 1 equiv of *i*-PrMgCl only yielded starting unreacted starting material after extractive workup, hence we decided to shed some light onto this behavior computationally. Our calculations predicted a complete selectivity

NIH-PA Author Manuscript

NIH-PA Author Manuscript

NIH-PA Author Manuscript

towards methoxy group substitution and activation barriers similar to those obtained for the analogous 1-methoxy-2-naphthoate (lowest energy barriers: $\Delta G^{\ddagger}_{OMe}$ = +19.9 for **7-TS$_{OMe}$** and $\Delta G^{\ddagger}_{C=O}$ = +27.1 kcal mol$^{-1}$ for **7-TS$_{C=O}$**, respectively).

Based on previous reports,[31] we envisaged the possible *in situ* formation of indenylmagnesium bromide[32] or bis(indenyl)magnesium[33,34] as the reason for this lack of reactivity with stoichiometric amount of Grignard reagent (the pKa of 1H-indene is 20.1 in dimethylsulfoxide[35]). According to this hypothesis and our predicted reactivity, we were glad to demonstrate that the treatment of **7** with 3 equiv of *i*-PrMgCl cleanly gave displacement of the methoxy group with no detectable attack to the carbonyl group in excellent yield (90%, Scheme 3). Interestingly, the activation barriers for the same reactions starting from the deprotonated and fully aromatic indenyl anion **7'**, are exceedingly high to be overcome at the reaction temperature (lowest energy barriers: $\Delta G^{\ddagger}_{OMe}$ = +44.5 for **7'-TS$_{OMe}$** and $\Delta G^{\ddagger}_{C=O}$ = +33.9 kcal mol$^{-1}$ for **7'-TS$_{C=O}$**, respectively), pointing to the remaining protonated 1Hindene in solution as the reactive species in this reaction.

The source of such a great difference between the two addition pathways in the 1H-indene derivative **7**, lies on the interruption of π-delocalization along the well-defined α,β-unsaturated system when the addition takes place to the carbonyl group, an issue that is alleviated in much more delocalized systems such as naphthalenes. The greater conjugation with respect to reactants achieved in the *ipso*-disubstituted adduct makes the 1,4-addition step more exergonic (ΔG = −14.7 kcal mol$^{-1}$) and the 1,2-addition less exergonic (ΔG = −10.0 kcal mol$^{-1}$) compared to the aromatic ester **1a** (ΔG = −7.3 and −12.7 kcal mol$^{-1}$, respectively).

As a general trend observed here, the lower energy TS for methoxy group displacement are earlier (*i.e.* close in geometry and energy to the reactants), in good agreement with Hammond's postulate[36] for exergonic processes. Thus, the $C_{OMe}$–$C_{Et}$ forming bond distance in the more stable **7-TS$_{OMe}$** derived from 1H-indene is longer (2.40 Å) than in the naphthalene-derived **1a-TS$_{OMe}$** (2.30 Å) whereas the $C_{C=O}$–$C_{Et}$ forming bond distance is slightly shorter in less stable in **7-TS$_{C=O}$** than in **1a-TS$_{C=O}$** (2.26 and 2.27 Å, respectively).

## Functional groups effects

The influence of both the nature and position of the reacting groups was demonstrated in our previous report.[1] Thus, a simple change in the location of the alkoxy group to provide other *ortho* isomer, namely methyl 3-methoxy-2-naphthoate **9**, disrupted its reactivity as demonstrated by competition experiments. In the course of our computational investigations to rationalize this reactivity, we found that although the methoxy displacement pathway was clearly disfavored using EtMgCl as Grignard reagent model (lowest energy barrier: $\Delta G^{\ddagger}_{OMe}$ = +30.8 for **9-TS$_{OMe}$**), the reactivity at the carbonyl group remained essentially unchanged (lowest energy barrier: $\Delta G^{\ddagger}_{OMe}$ = +22.1 for **9-TS$_{C=O}$**), providing a complete chemoselectivity towards 1,2-addition.

The change of primary EtMgGl by secondary *i*-PrMgCl, which was the Grignard reagent used experimentally, did not change this trend (lowest energy barriers: $\Delta G^{\ddagger}_{OMe}$ = +30.4 for **9'-TS$_{OMe}$** and $\Delta G^{\ddagger}_{C=O}$ = +22.4 kcal mol$^{-1}$ for **9'-TS$_{C=O}$**, respectively). These theoretical results were not in accordance with the reported reactivity for this substrate, since a slower but still complete chemoselectivity towards methoxy group displacement was previously published.[1] Intrigued by these observations, we repeated the same reactions and re-examined the NMR data of the isolated compounds carefully. Thereafter, we concluded that our previous assessment of reactivity for this compound was wrong, and the ester carbonyl group indeed reacts exclusively to provide the corresponding isopropyl ketone **10** in good yield (85%, Scheme 4), which did not undergo further 1,2-addition.

NIH-PA Author Manuscript

NIH-PA Author Manuscript

NIH-PA Author Manuscript

These new results predicted by the computations gave rise to a correction of the original manuscript and stress the great benefits of integrating experiments and calculations.

The reduced reactivity of the methoxy group at the 3 position in compound **9** is again reflected by the late character (structurally close to the product) of the corresponding 1,4-addition TS illustrated by the short $C_{OMe}$– $C_{alkyl}$ forming bond distance (2.17 Å with EtMgCl and 2.23 Å with *i*-PrMgCl, Figure 4). Moreover, this methoxy group displacement proceeded in an asynchronous but concerted manner without the formation of a stable tetrahedral intermediate, as revealed by IRC calculations. The origin of this lower reactivity is the poorer ability of 3-methoxy-2-naphthoates to stabilize the formal negative charge generated after 1,4-addition of the alkyl group with respect to 1-methoxy-2-naphthoates (Figure S2 in Supporting Information). The lack of resonance structures preserving the aromaticity of one fused benzene ring precludes the formation of stable adducts after 1,4-addition and drives the concerted elimination of the methoxy group in order to recover naphthalene aromaticity. Additionally, and as can be seen in Figure 4, the contribution of the *ipso* carbon bearing the methoxy group to the LUMO of 3-methoxy-2-naphthoate **9** is almost negligible in opposition to 1-methoxy isomer **1a**, justifying the complete selectivity towards 1,2-carbonyl addition with Grignard reagents of the former.

As described in our previous study,[1] the presence of a theoretically better leaving group than alkoxide (such as tosylate) completely inhibits the displacement reaction at low temperature, even with primary nucleophiles like *n*-BuMgCl and *i*-BuMgCl. This apparently counterintuitive result was rationalized computationally by a higher calculated activation barrier for mesylate (simpler model of tosylate) displacement using EtMgCl as Grignard model (lowest energy barrier: $\Delta G^{\ddagger}_{OMe}$ = +25.6 for **11-TS$_{OMe}$**) with respect to methoxy substitution in analogous compounds. Reversing the trend calculated for similar alkoxy derivatives, the nucleophilic addition of the same reactant to the carbonyl group is now *ca.* 4 kcal mol$^{-1}$ lower in energy (lowest energy barrier: $\Delta G^{\ddagger}_{C=O}$ = +21.8 for **11-TS$_{C=O}$**), which provides complete chemoselectivity towards this pathway. To our delight, when the reaction mixture was allowed to reach room temperature overnight, only addition to the ester carbonyl group of **11** towards the corresponding tertiary alcohol **12** was observed, as predicted by our calculations, albeit with low conversion and in low yield (20%, Scheme 5).

The decreased propensity of tosylate group to be displaced lies in its inability to form a stable six-membered chelate involving the oxygen attached to the *ipso* carbon (**11•EtMgCl_a**) as in the methoxy-substituted analogues. Instead, the carbonyl oxygen and a sulfonyl oxygen form an eight-membered chelate (**11•EtMgCl_b**), which promotes the activation of only the ester group towards nucleophilic addition (Figure 5). Due to the weaker coordinating character of sulfonate esters compared to ethers, these chelates are significantly less stable ($\Delta G_{complex}$ = +7.5 and −0.2 kcal mol$^{-1}$, respectively) than the 1-methoxysubstitued analogue.

Although ketones are generally viewed as incompatible with the high nucleophilicity of Grignard reagents, we have shown that the displacement reaction is facile at temperatures below which the ester or ketone products will undergo addition (Table 1, entries 2–5)[1]. As an exception, MeMgI in $CH_2Cl_2$ undergoes complete addition to the carbonyl group as previously reported[31] and confirmed in our lab (Table 1, entry 1). In this sense, computations on the reaction of methylketone **13a** with EtMgCl reproduced this trend quantitatively by estimating a 77:23 ratio favoring the displacement of the methoxy group with EtMgCl (lowest energy barriers: $\Delta G^{\ddagger}_{OMe}$ = +19.0 for **13a-TS$_{OMe}$** and $\Delta G^{\ddagger}_{C=O}$ = +19.5 kcal mol$^{-1}$ for **13a-TS$_{C=O}$**, respectively). Interestingly, the simple change of methyl group in the ketone by a *n*-butyl group in **13b**, produces an increase in the calculated selectivity, providing a calculated ratio of 95:5 towards 1,4-conjugate addition, in very good

NIH-PA Author Manuscript

NIH-PA Author Manuscript

NIH-PA Author Manuscript

agreement with experimental observations (lowest energy barriers: $\Delta G^{\ddagger}_{OMe}$ = +19.6 for **13b-TS$_{OMe}$** and $\Delta G^{\ddagger}_{C=O}$ = +20.5 kcal mol$^{-1}$ for **13b-TS$_{C=O}$**, respectively). Moreover, and somewhat unexpectedly, the computations on the reaction of methyl ketone **13a** with a slightly harder nucleophile such as MeMgCl also reproduced the experimentally observed inversion of chemoselectivity, providing a calculated 9:91 ratio towards the formation of the corresponding tertiary alcohol (lowest energy barriers: $\Delta G^{\ddagger}_{OMe}$ = +22.0 for **13a-TS'$_{OMe}$** and $\Delta G^{\ddagger}_{C=O}$ = +21.1 kcal mol$^{-1}$ for **13a-TS'$_{C=O}$**, respectively).

As mentioned before, the more stable TS´s for 1,4-addition on 1-methoxy-2-naphthyl methyl ketone **13a** are earlier as reflected by the $C_{OMe}$–$C_{Et}$ forming bond distances (2.38 Å and 2.28 Å with EtMgCl and MeMgCl, respectively).

These results stress the great importance of properly choosing the substrate models for the calculations, because very similar EtMgCl and MeMgCl provide very different reactivity patterns.

The reaction with more reactive carbonyls such as aldehydes completely changes the general selectivity trend observed with less electrophilic vinylogous esters and ketones. According to the experimental results (Table 1, entry 6),[1] the chemoselectivity calculated for the addition of EtMgCl (computational model *n*-BuMgCl) to 1-methoxy-2-naphthaldehyde **13c** is reversed with respect to analogous ester **1a** with a calculated ratio of 2:98 favoring the attack towards the carbonyl group. As can be seen in Figure 7, the contribution of the carbonyl carbon to the LUMO is larger in naphthyl aldehyde **13c** than in the analogous methyl ester **1a**, justifying the higher selectivity towards 1,2 carbonyl addition with Grignard reagents of the former. It is noteworthy that the activation energies for both competitive pathways decrease significantly in the case of aromatic aldehydes (lowest energy barriers: $\Delta G^{\ddagger}_{OMe}$ = +16.8 kcal mol$^{-1}$ for **13c-TS$_{OMe}$** and $\Delta G^{\ddagger}_{C=O}$ +15.4 kcal mol$^{-1}$ for **13c-TS$_{C=O}$**, respectively). Interestingly, this decrease in the activation barriers matches the lower stability of the reactant complex with weaker coordinating aldehydes (**13c•EtMgCl**, $\Delta G_{complex}$ = +0.1 kcal mol$^{-1}$), which are essentially thermoneutral and 6–7 kcal mol$^{-1}$ less stable that those of the corresponding vinylogous esters and ketones. The TS's for both nucleophilic additions in **13c**, are the earliest of all calculated species, exhibiting the largest $C_{OMe}$–$C_{Et}$ and $C_{C=O}$–$C_{Et}$ forming bonds distances (2.42 Å and 2.55 Å, respectively).

## The role of magnesium chelate

In previously reported reactions similar to those described herein, the formation of stable transient chelate complexes with organoalkyl reagents prior to nucleophilic akyl transfer has been proposed.[22–24]

The key role of magnesium in this type of reactivity is reflected by the numerous examples reported, for instance, for the conversion of esters into ketones in the presence of alkoxy groups susceptible of displacement.[37–41]

In our calculations, satisfactory activation barriers and chemoselectivities were obtained from quite stable complexes between alkyl Grignards and bidentate *ortho*-methoxycarbonyl species. To further investigate the role of these complexes in the reaction outcome, we calculated the same reaction profiles starting from alternative monodentate structures with $CH_3MgCl$, adding a solvent molecule (DME) to achieve a comparable coordination environment around magnesium and prevent chelation (Figure 8a). Any attempt to locate methoxy-coordinated non-chelated structures was unsuccessful even if an alternate ester rotamer was considered. Notably, the reactant complex in which the magnesium adopts a pentacoordinated environment by coordinating to both the methoxy and carboxyl oxygen

NIH-PA Author Manuscript

NIH-PA Author Manuscript

NIH-PA Author Manuscript

atoms, is significantly less stable than the tetrahedral monodentante complex with the carbonyl group ($\Delta G_{complex}$ = +2.9 kcal mol$^{-1}$ for **1'a•$CH_3MgCl$(DME))**, which in turn is much less stable than the Mg-carbonyl-ether chelated species discussed above. The energy barrier for methoxy displacement increases by *ca.* 13 kcal mol$^{-1}$ with respect to the unsolvated chelate, but the activation energy for 1,2 addition to the carbonyl group remains essentially unperturbed.

Finally, in an attempt to completely dissect the contribution of the methoxy and ester groups to the observed reactivity, we calculated the energy profiles starting from monosubstituted 1-methoxynaphthalene **16** and methyl 2-naphthoate **17**, including again a solvent molecule to provide tetracoordination for magnesium (Figure 8b). The monodentate complexes of these species with $CH_3MgCl$ resulted to be quite unstable compared to the chelated ones, specially the methoxy-derived species ($\Delta G_{complex}$ = +14.4 kcal mol$^{-1}$ for **16•$CH_3MgCl$(DME)** and $\Delta G_{complex}$ = +2.6 kcal mol$^{-1}$ for **17•$CH_3MgCl$(DME))**. Moreover, the activation barrier for methoxy group displacement is totally unfeasible ($\Delta G^{\ddagger}_{OMe}$ = +55.9 for **16-$TS_{OMe}$ (DME))**, and virtually identical to those previously calculated for 1,2 ester carbonyl attack ($\Delta G^{\ddagger}_{C=O}$ = +25.1 for **17-$TS_{C=O}$ (DME)**).

Altogether, these results clearly indicate that the presence of a carbonyl group is required to achieve alkoxy group displacement with Grignard reagents, as ethers themselves are not able to efficiently coordinate to the Lewis acid. The presence of a chelate complex does not appear to be mandatory for carbonyl activation, whereas the methoxy group is completely unreactive in the absence of the chelate even if magnesium is (poorly) coordinated to the alkoxy group oxygen. The true 1,4-conjugate addition character of the initial steps of methoxy group displacement is revealed through these results.

Thus, the presence of an acyl group in *ortho* position of the aromatic system allows both the Lewis acid-enhanced activation of the β position of the α,β-unsaturated carbonyl system, and the stabilization of the negative charge generated upon alkyl addition in the form of magnesium enolates, which ultimately triggers the displacement reaction.

## Conclusions

An inner-sphere mechanism through metalaoxetane-like TS has been determined computationally for the displacement of alkoxy groups of vinylogous esters and ketones by Grignard reagents. The formation of a stable organomagnesium chelate between both oxygenated groups allows this reaction to take place, which is otherwise inaccessible, even in the presence of expectedly better leaving groups such as tosylate. The calculated chemoselectivities towards 1,4-conjugate (with esters and ketones) or 1,2-addition (with aldehydes) are in excellent agreement with the experimental results and rationalize the influence of the nature and position of both the leaving alkoxy and adjacent carbonyl groups. The reasons behind the different reactivities are the modification of the substrate LUMO by the *ortho* carbonyl group, and the ability of the substrates to stabilize the negative charge by π-delocalization after nucleophilic addition. Our computational predictions were verified experimentally, leading in some cases to the reinterpretation of previous experimental results as in the reaction of two position isomers of the same methyl alkoxynaphthanoate.

## Experimental Section

### Computational Details

All calculations were carried out with the B3LYP hybrid functional[42,43] and 6-31G(d) basis set. Full geometry optimizations and transition structure (TS) searches were carried out with the Gaussian 09 package.[44] The possibility of different conformations was taken into

NIH-PA Author Manuscript

NIH-PA Author Manuscript

NIH-PA Author Manuscript

account for all structures. The theoretical ratio of reaction products was obtained through the energy of the different transition states using a Maxwell–Boltzmann distribution at −78 °C, temperature at which thermal and entropic corrections to energy were calculated. Frequency analyses were carried out at the same level used in the geometry optimizations, and the nature of the stationary points was determined in each case according to the appropriate number of negative eigenvalues of the Hessian matrix. The harmonic oscillator approximation in the calculation of vibration frequencies was replaced by the quasiharmonic approximation developed by Cramer and Truhlar.[45] Scaled frequencies were not considered since significant errors in the calculated thermodynamic properties are not found at this theoretical level.[46,47] Where necessary, mass-weighted intrinsic reaction coordinate (IRC) calculations were carried out by using the Gonzalez and Schlegel scheme[48,49] in order to ensure that the TSs indeed connected the appropriate reactants and products. Bulk solvent effects were considered implicitly by performing single-point energy calculations on the gas-phase optimized geometries, through the SMD polarizable continuum model of Cramer and Thrular[50] as implemented in Gaussian 09. The internally stored parameters for tetrahydrofuran were used to calculate solvation free energies ($\Delta G_{solv}$). Gibbs free energies ($\Delta G$) were used for the discussion on the relative stabilities of the considered structures. Cartesian coordinates, electronic energies, entropies, enthalpies, Gibbs free energies, lowest frequencies of the different conformations of all structures considered are available as Supporting Information.

## Materials

Unless otherwise specified, all commercially available reagents were used as received. All reactions using dried solvents were carried out under an atmosphere of argon in flame-dried glassware with magnetic stirring. Dry solvent was dispensed from a solvent purification system that passes solvent through two columns of dry neutral alumina. Silica gel chromatographic purifications were performed by flash chromatography with silica gel (sigma, grade 62, 60–200 mesh) packed in glass columns; the eluting solvent for each purification was determined by thin layer chromatography (TLC). Analytical TLC was performed on glass plates coated with 0.25 mm silica gel using UV for visualization.

## Instrumentation

$^{1}$H NMR spectra were obtained on a 300 MHz, 400 MHz or a 600 MHz NMR spectrometer. Chemical shifts (δ) are reported in parts per million (ppm) relative to residual solvent (CHCl3, s, δ 7.26). Multiplicities are given as: s (singlet), d (doublet), t (triplet), q (quartet), dd (doublet of doublets), sep (septuplet), m (multiplet). Proton-decoupled $^{13}$C NMR spectra were obtained on a 75 MHz, 101 MHz, or a 150 MHz NMR spectrometer. $^{13}$C chemical shifts are reported relative to $CDCl_3$ (δ 77.2 ppm). IR frequencies are given in $cm^{-1}$ and spectra were obtained on a FT-IR spectrometer equipped with a DTGS detector and diamond ATR accessory. High-resolution mass spectra were obtained on an Orbitrap FTMS.

## Synthesis of methyl 1-methyl-2-naphthoate (2a)

To a cooled solution (−78 °C) of **1a** (1.55 g, 7.19 mmol) in 36 mL of $CH_2Cl_2$ was added a solution of $CH_3MgI$ in Et2O (3.0 M, 2.4 mL). The reaction was monitored until complete by TLC and quenched with saturated ammonium chloride (5 mL). The resulting layers were separated, and the aqueous layer was extracted with 2×10 mL of EtOAc. The combined organic layers were washed with 20 mL of brine, dried ($MgSO_4$), and concentrated *in vacuo* to afford the crude product mixture. Integration of the crude NMR indicated a 83:17 ratio of **2a** to **15a**. The product was purified by flash chromatography (5:95 EtOAc/hexanes) to afford the product **2a** as a white solid (0.72 g, 50%): m.p. = 55-56 °C; $^{1}$H NMR (600 MHz, CDCl3) δ 8.19 (d, *J* = 9.0 Hz, 1H), 7.84 (m, 2H), 7.72 (d, *J* = 8.5 Hz, 1H), 7.57 (m, 2H),

NIH-PA Author Manuscript

NIH-PA Author Manuscript

NIH-PA Author Manuscript

3.97 (s, 3H), 2.95 (s, 3H); $^{13}$C NMR (151 MHz, $CDCl_3$) 169.2, 137.1, 134.6, 132.8, 128.5, 127.8, 127.3, 126.5, 126.1, 125.8, 125.3, 52.1, 15.8; HRMS (ammonia CI) m/z calcd for $C_{13}H_{16}NO_2$ $(M + NH4)^+$ 218.1181, found 218.1183; IR (thin film) 3090, 2954, 1685 and demethylated byproduct methyl 1-hydroxy-2-naphthoate **18** (0.07 g, 5%) $^1$H NMR values matched those previously reported. The tertiary alcohol **15a** was unable to be chromatographically separated from a small amount of residual starting material. An analytically pure sample used a reference for integration of the crude NMR was prepared from the corresponding ketone **13a**.

### Synthesis of methyl 3-isopropyl-1H-indene-2-carboxylate (8)

To a cooled solution (−78 °C) of **7** (1.14 g, 5.58 mmol) in 28 mL of THF was added a solution of *i*-PrMgCl in Et2O (2.0 M, 8.37 mL) The reaction was monitored until complete by TLC and quenched with saturated ammonium chloride (5 mL). The resulting layers were separated, and the aqueous layer was extracted with 2×10 mL of EtOAc. The combined organic layers were washed with 20 mL of brine, dried ($MgSO_4$), and concentrated *in vacuo* to afford the crude displacement product. The product was purified by flash chromatography (5:95 EtOAc/hexanes) to afford the product **8** as a yellow solid (1.08 g , 90%): m.p. = 79-80 °C; $^1$H NMR (600 MHz, $CDCl_3$) δ 7.78 (m, 1H), 7.50 (m, 1H), 7.33 (m, 2H), 4.31(m, 1H), 3.84 (s, 3H), 3.66 (s, 2H), 1.45 (d, $J$ = 7.2 Hz, 6H); $^{13}$C NMR (151 MHz, $CDCl_3$) δ 166.3, 161.2, 144.4, 143.0, 128.3, 127.2, 126.1, 124.4, 123.7, 51.2, 39.2, 26.7, 20.9; HRMS (ammonia CI) m/z calcd for $C_{14}H_{17}O_2$ $(M + H)^+$ 217.1223, found 217.1233; IR (thin film) 3075, 2975, 1710.

### Synthesis of 2-(4-hydroxy-2,6-dimethylheptan-4-yl)naphthalen-1-yl 4-methylbenzenesulfonate (12)

To a cooled solution (−78 °C) of tosylate **11** (0.23 g, 0.63 mmol) in 3.15 mL of $CH_2Cl_2$ was added a solution of *i*-BuMgCl in $Et_2O$ (2.0 M, 0.32 mL) The reaction was then stirred for 18 h during which time the solution was allowed to warm to room temperature. The reaction was quenched with saturated ammonium chloride (10 mL). The resulting layers were separated, and the aqueous layer was extracted with 2×10 mL of $CH_2Cl_2$. The combined organic layers were washed with 20 mL of brine, dried ($MgSO_4$), and concentrated *in vacuo* to afford the crude product. The product was purified by flash chromatography (5:95 EtOAc/hexanes) to afford the product 12 as a colorless oil (0.056 g, 20%). $^1$H NMR (600 MHz, $CDCl_3$) δ 7.98 (d, $J$ = 8.3 Hz, 2H), 7.80 – 7.76 (m, 2H), 7.72 (d, $J$ = 8.8 Hz, 1H), 7.53 (d, $J$ = 8.7 Hz, 1H), 7.44 (ddd, $J$ = 8.1, 6.8, 1.1 Hz, 1H), 7.41 (d, $J$ = 8.1 Hz, 2H), 7.34 (ddd, $J$ = 8.3, 6.8, 1.2 Hz, 1H), 2.51 (s, 3H), 2.10 (dd, $J$ = 14.5, 5.2 Hz, 2H), 1.78 (dd, $J$ = 14.5, 6.6 Hz, 2H), 1.69 (m, 2H), 0.94 (d, $J$ = 6.6 Hz, 6H), 0.75 (d, $J$ = 6.6 Hz, 6H). $^{13}$C NMR (151 MHz, $CDCl_3$) δ 145.4, 142.5, 137.1, 134.0, 133.6, 129.9, 128.9, 128.3, 127.3, 126.8, 126.6, 126.3, 123.2, 79.8, 51.9, 24.5, 24.3, 21.8, 18.6; HRMS (ESI) m/z calcd for $C_{26}H_{32}NaO_4S$ $(M + Na)^+$ 463.1919, found 463.1921; IR (thin film) 3415, 3065, 2950, 1580.

### Synthesis of 2-(1-methoxynaphthalen-2-yl)propan-2-ol (15a)

To a cooled solution (−78 °C) of **13a** (1.86 g, 9.30 mmol) in 50 mL of $CH_2Cl_2$ was added a solution of MeMgI in $Et_2O$ (3.0 M, 3.1 mL). The reaction was monitored until complete by TLC and quenched with saturated ammonium chloride (5 mL). The resulting layers were separated, and the aqueous layer was extracted with 2×10 mL of EtOAc. The combined organic layers were washed with 20 mL of brine, dried ($MgSO_4$), and concentrated *in vacuo* to afford the crude product mixture. The product was purified by flash chromatography (5:95 EtOAc/hexanes) to afford the product **15a** as a clear oil (0.71 g, 35%): $^1$H NMR (600 MHz, $CDCl_3$) δ 8.07 (d, $J$ = 8.3 Hz, 1H), 7.83 (d, $J$ = 8.1 Hz, 1H), 7.60 (d, $J$ = 8.6 Hz, 1H), 7.51(m, 3H), 4.07 (s, 3H), 1.73 (s, 6H); (600 MHz, CDCl3) δ 152.7, 136.1, 134.3, 128.1,

NIH-PA Author Manuscript

NIH-PA Author Manuscript

NIH-PA Author Manuscript

127.9, 126.0, 125.9, 124.6, 124.2, 122.1, 73.6, 63.3, 31.8; HRMS (ammonia CI) m/z calcd for $C_{14}H_{15}O$ $(M + H - H_2O)^+$ 199.1123, found 199.1132; IR (thin film) 3420, 3066, 2957, 1586.

## Supplementary Material

Refer to Web version on PubMed Central for supplementary material.

## Acknowledgments

This research was supported by National Science Fundation (CHE-1059084 to K.N.H.) the Petroleum Research Fund (administered by the American Chemical Society) and by the National Institutes of Health (R56AI80931-01 and R01AI080931-01 to J.T.S.). G.J.O acknowledges Ministerio de Economía y Competitividad (EX2010-1063 postdoctoral grant) and A.J.B for support in the form of a Bradford Borge Graduate Research Fellowship from UC Davis. Calculations were performed on the Hoffman2 cluster at UCLA and the Extreme Science and Engineering Discovery Environment (XSEDE), which is supported by the National Science Foundation (OCI-1053575). We thank Dr. Jesús García-López for useful discussions.

## REFERENCES

1. Brockway A, González-López M, Fettinger JC, Shaw JT. J. Org. Chem. 2011; 76:3515–3518. [PubMed: 21446670]
2. Fuson RC, Speck SB. J. Am. Chem. Soc. 1942; 64:2446–2448.
3. Fuson RC, Wassmundt FW. J. Am. Chem. Soc. 1956; 78:5409–5413.
4. Rice JE, He ZM. J. Org. Chem. 1990; 55:5490–5494.
5. Rice JE, Shih HC, Hussain N, LaVoie EJ. J. Org. Chem. 1987; 52:849–855.
6. Hotta H, Suzuki T, Miyano S. Chem. Lett. 1990; 19:143–144.
7. Parker JS, Smith NA, Welham MJ, Moss WO. Org. Process Res. Dev. 2003; 8:45–50.
8. Hattori T, Suzuki T, Miyano S. J. Chem. Soc. Chem. Commun. 1991:1375–1376.
9. Hattori T, Suzuki T, Hayashizaka N, Koike N, Miyano S. Bull. Chem. Soc. Jpn. 1993; 66:3034–3040.
10. Hattori T, Koike N, Miyano S. J. Chem. Soc. Perkin Trans. 1994; 1:2273–2282.
11. Hattori T, Shimazumi Y, Goto H, Yamabe O, Morohashi N, Kawai W, Miyano S. J. Org. Chem. 2003; 68:2099–2108. [PubMed: 12636367]
12. Meyers AI, Mihelich ED. J. Am. Chem. Soc. 1975; 97:7383–7385.
13. Meyers AI, Gabel R, Mihelich ED. J. Org. Chem. 1978; 43:1372–1379.
14. Meyers AI, Avila WB. J. Org. Chem. 1981; 46:3881–3886.
15. Meyers AI, Lutomski KA. J. Am. Chem. Soc. 1982; 104:879–881.
16. Meyers AI, Lutomski KA. Synthesis. 1983; 1983:105–107.
17. Patten AD, Nguyen Nhan H, Danishefsky SJ. J. Org. Chem. 1988; 53:1003–1007.
18. Wilson JM, Cram DJ. J. Am. Chem. Soc. 1982; 104:881–884.
19. Meyers AI, Flisak JR, Aitken RA. J. Am. Chem. Soc. 1987; 109:5446–5452.
20. Rizzacasa MA, Sargent MV. J. Chem. Soc. Chem. Commun. 1990:894–896.
21. Meyers AI, Willemsen JJ. Tetrahedron. 1998; 54:10493–10511.
22. Reetz MT, Keßeler K, Schmidtberger S, Wenderoth B, Steinbach R. Angew. Chem. Int. Ed. Engl. 1983; 22:1511–1526.
23. Tamai Y, Hattori T, Date M, Koike S, Kamikubo Y, Akiyama M, Seino K, Takayama H, Oyama T, Miyano S. ChemInform. 1999; 30:1–1.
24. Keck GE, Castellino S. J. Am. Chem. Soc. 1986; 108:3847–3849.
25. Ashby EC, Smith MB. J. Am. Chem. Soc. 1964; 86:4363–4370.
26. Spek AL, Voorbergen P, Schat G, Blomberg C, Bickelhaupt F. J. Organomet. Chem. 1974; 77:147–151.

NIH-PA Author Manuscript

NIH-PA Author Manuscript

NIH-PA Author Manuscript


27. Avent AG, Caro CF, Hitchcock PB, Lappert MF, Li Z, Wei XH. Dalton Trans. 2004:1567–1577. [PubMed: 15252606]
28. Ellison JJ, Power PP. J. Organomet. Chem. 1996; 526:263–267.
29. Schlenk W, Schlenk W. Berichte d. D. Chem. Gesellschaft. 1929; 62:920–924.
30. Ashby EC. Q. Rev. Chem. Soc. . 1967; 21:259–285.
31. Watanabe N, Nagamatsu K, Mizuno T, Matsumoto M. Luminescence. 2005; 20:63–72. [PubMed: 15803504]
32. Ford WT, Radue R, Walker JA. J. Chem. Soc. D. 1970:966–967.
33. Gritzo H, Schaper F, Brintzinger HH. Acta Crystallogr. Sect. E: Struct. Rep. Online. 2004; 60:m1108–m1110.
34. Atwood JL, Smith KD. J. Am. Chem. Soc. 1974; 96:994–998.
35. Bordwell FG. Acc. Chem. Res. 1988; 21:456–463.
36. Hammond GS. J. Am. Chem. Soc. 1955; 77:334–338.
37. Yamaguchi M, Nakamura S, Okuma T, Minami T. Tetrahedron Lett. 1990; 31:3913–3916.
38. Jeong JH, Weinreb SM. Org. Lett. 2006; 8:2309–2312. [PubMed: 16706513]
39. Kraus GA, Wie J, Thite A. Synthesis. 2008; 2008:2427–2431.
40. Laatsch H, Pudleiner H. Liebigs Ann. Chem. 1989; 1989:863–881.
41. Carpenter TA, Evans GE, Leeper FJ, Staunton J, Wilkinson MR. J. Chem. Soc. Perkin Trans. 1984; 1:1043–1051.
42. Lee C, Yang W, Parr RG. Phys. Rev. B: Condens. Matter Mater. Phys. 1988; 37:785–789.
43. Becke AD. J. Chem. Phys. 1993; 98:5648–5652.
44. Frisch, MJ.; Trucks, GW.; Schlegel, HB.; Scuseria, GE.; Robb, MA.; Cheeseman, JR.; Scalmani, G.; Barone, V.; Mennucci, B.; Petersson, GA.; Nakatsuji, H.; Caricato, M.; Li, X.; Hratchian, HP.; Izmaylov, AF.; Bloino, J.; Zheng, G.; Sonnenberg, JL.; Hada, M.; Ehara, M.; Toyota, K.; Fukuda, R.; Hasegawa, J.; Ishida, M.; Nakajima, T.; Honda, Y.; Kitao, O.; Nakai, H.; Vreven, T.; JA Montgomery, J.; Peralta, JE.; Ogliaro, F.; Bearpark, M.; Heyd, JJ.; Brothers, E.; Kudin, KN.; Staroverov, VN.; Kobayashi, R.; Normand, J.; Raghavachari, K.; Rendell, A.; Burant, JC.; Iyengar, SS.; Tomasi, J.; Cossi, M.; Rega, N.; Millam, JM.; Klene, M.; Knox, JE.; Cross, JB.; Bakken, V.; Adamo, C.; Jaramillo, J.; Gomperts, R.; Stratmann, RE.; Yazyev, O.; Austin, AJ.; Cammi, R.; Pomelli, C.; Ochterski, JW.; Martin, RL.; Morokuma, K.; Zakrzewski, VG.; Voth, GA.; Salvador, P.; Dannenberg, JJ.; Dapprich, S.; Daniels, AD.; Farkas, Ö.; Foresman, JB.; Ortiz, JV.; Cioslowski, J.; Fox, DJ. Gaussian 09, Revision C.1. Wallingford CT: Gaussian, Inc.; 2009.
45. Ribeiro RF, Marenich AV, Cramer CJ, Truhlar DG. J. Phys. Chem. B. 2011; 115:14556–14562. [PubMed: 21875126]
46. Bauschlicher CW Jr. Chem. Phys. Lett. 1995; 246:40–44.
47. Merrick JP, Moran D, Radom L. J. Phys. Chem. A. 2007; 111:11683–11700. [PubMed: 17948971]
48. Gonzalez C, Schlegel HB. J. Chem. Phys. 1989; 90:2154–2161.
49. Gonzalez C, Schlegel HB. J. Phys. Chem. 1990; 94:5523–5527.
50. Marenich AV, Cramer CJ, Truhlar DG. J. Phys. Chem. B. 2009; 113:6378–6396. [PubMed: 19366259]

NIH-PA Author Manuscript
NIH-PA Author Manuscript
NIH-PA Author Manuscript



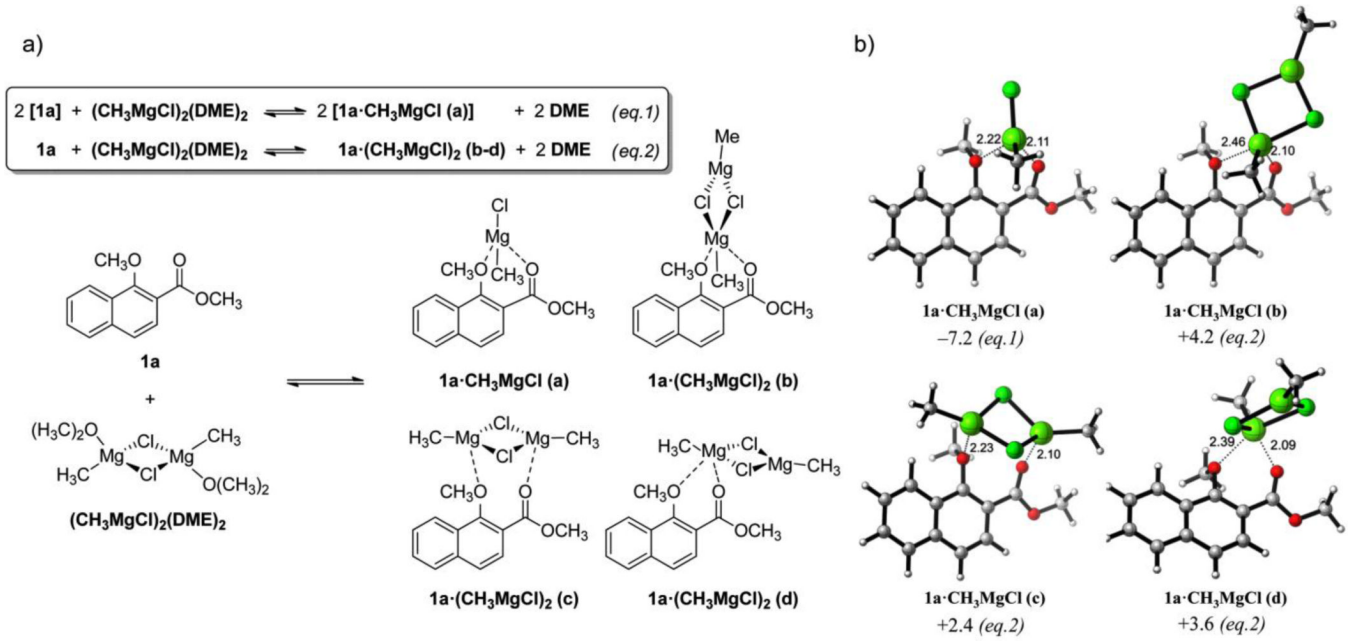


**Figure 1.**

a) Proposed coordination of Grignard reagents to vinylogous 1,2-alkoxy carbonyl compounds leading to 1:1 and 2:1 complexes (eq. 1 and eq. 2, respectively). Additional coordination modes are described in the Supporting Information. b) Structures and complexation free energies ($\Delta G_{complex}$) calculated at the PCM($CH_2Cl_2$)/B3LYP/6-31G(d) level. Energies are in kcal $mol^{-1}$ and distances are in Angstrom.

NIH-PA Author Manuscript
NIH-PA Author Manuscript
NIH-PA Author Manuscript



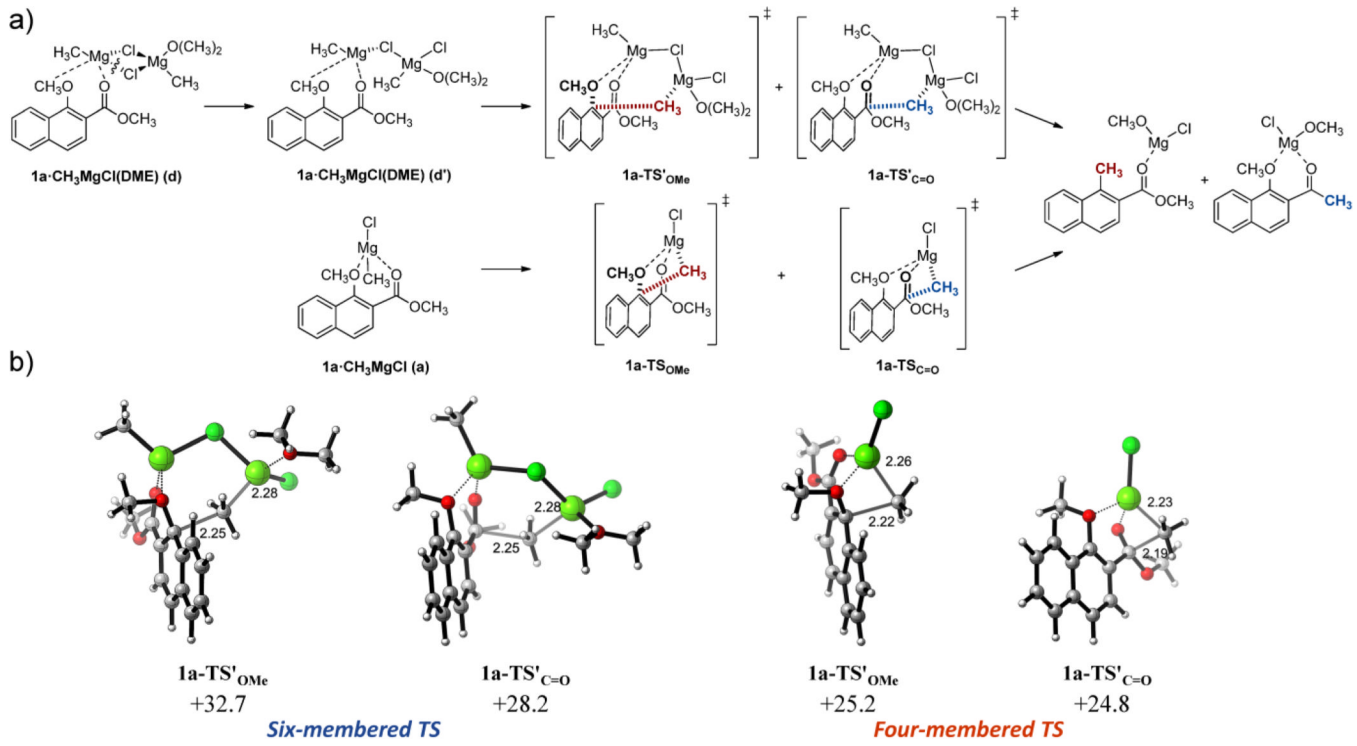


**Figure 2.**

a) Proposed mechanisms for the reaction of vinylogous 1,2-alkoxy carbonyl compounds with Grignard reagents through six-membered (TS') and four-membered (TS) cyclic transition states. b) Most relevant structures and activation free energies ($\Delta G^{\ddagger}$) calculated at the PCM($CH_2Cl_2$)/B3LYP/6-31G(d) level. Energies are in kcal $mol^{-1}$ and distances are in Angstrom.

NIH-PA Author Manuscript
NIH-PA Author Manuscript
NIH-PA Author Manuscript



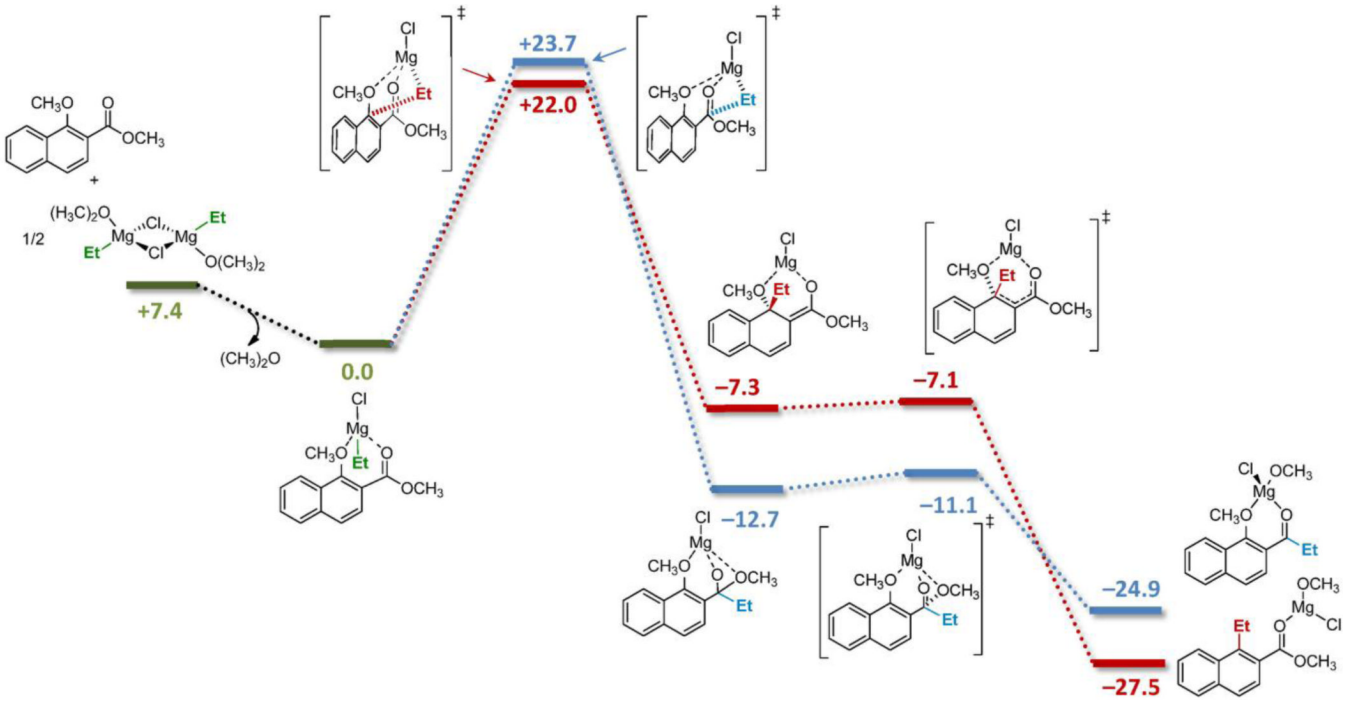


**Figure 3.**

Reaction pathways for the addition of Grignard reagents to aromatic 1,2-alkoxy esters calculated at the PCM(CH2Cl2)/B3LYP/6-31G(d) level. Free energies (ΔG) relative to the reactant complex are in kcal $mol^{-1}$.

NIH-PA Author Manuscript

NIH-PA Author Manuscript

NIH-PA Author Manuscript

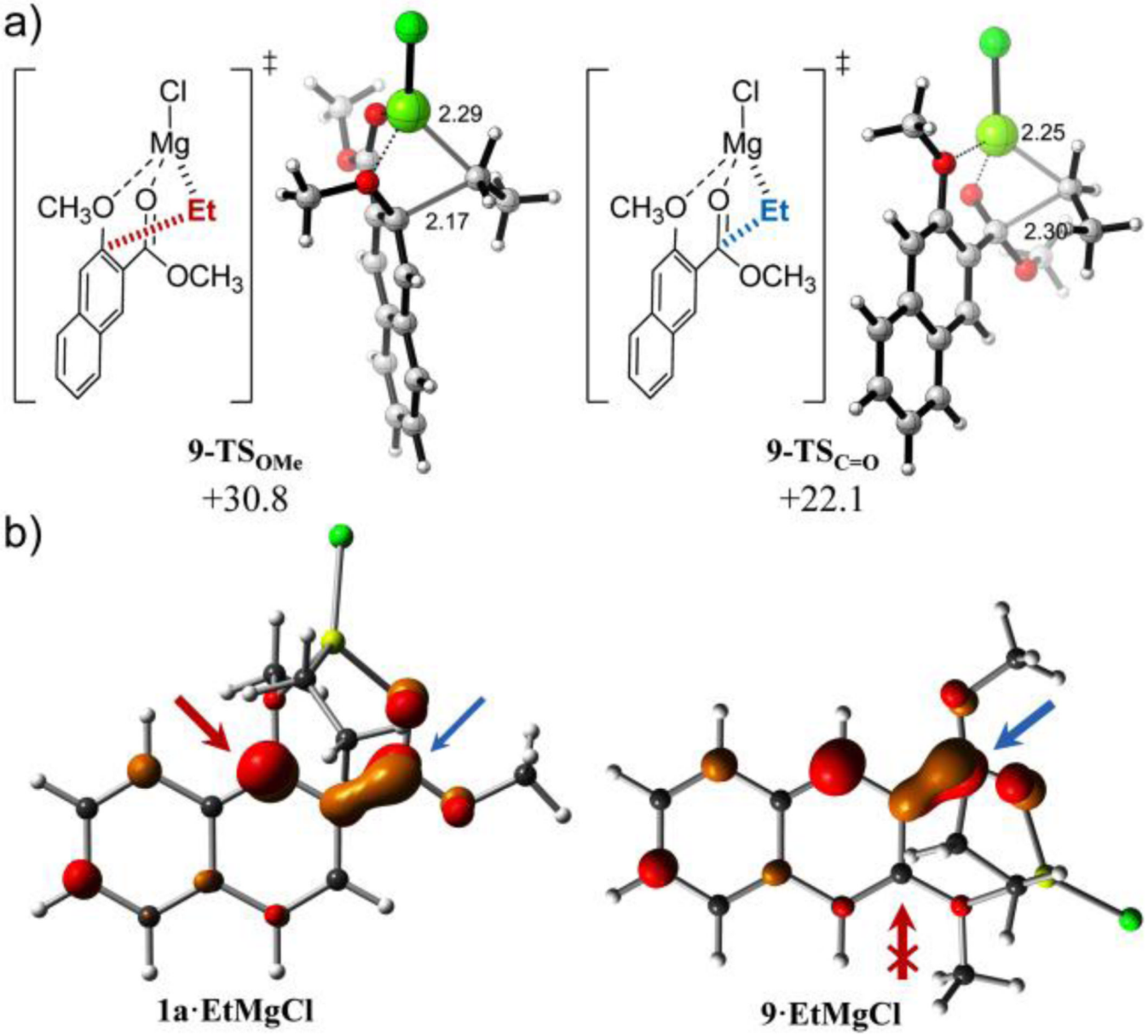


**Figure 4.**

a) Lowest-energy transition structures and activation free energies ($\Delta G^{\ddagger}$) for the reaction of naphthyl ester **9** and EtMgCl calculated at the PCM($CH_2Cl_2$)/B3LYP/6-31G(d) level. Energies are in kcal $mol^{-1}$ and distances are in Angstrom. b) Isosurface representation of LUMO of reactant complexes of isomers **1a** and **9**. Potentially reactive positions are marked with red (methoxy group) and blue (carbonyl group) arrows.

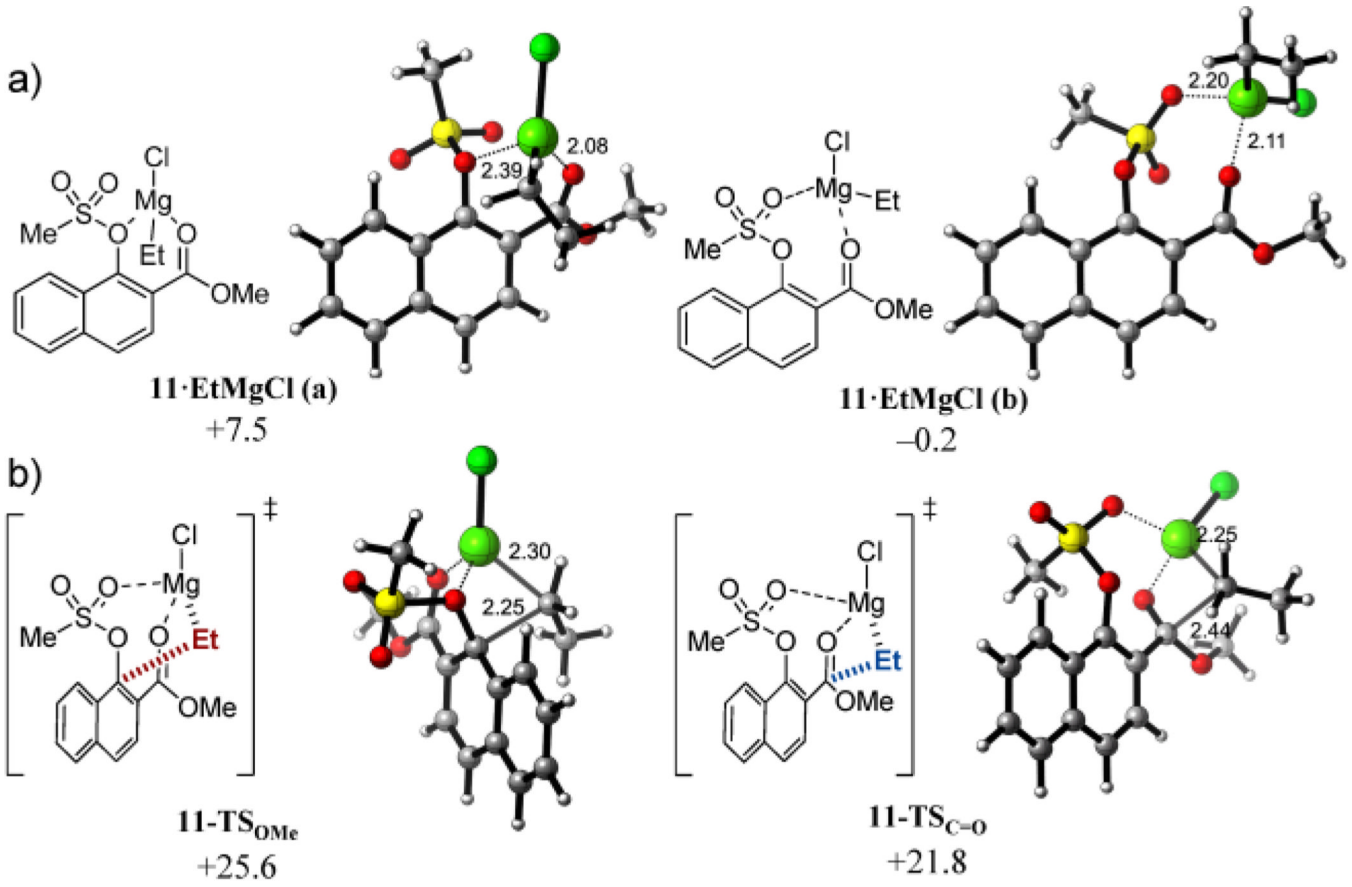


**Figure 5.**

a) Six-membered (left) and eight-membered (right) chelate reactant complexes of (mesyl)naphthyl ester **11** with EtMgCl together with their respective complexation free energies ($\Delta G_{complex}$). b) Lowest-energy transition structures and activation free energies ($\Delta G^{\ddagger}$) for the reaction of **11** and EtMgCl calculated at the PCM($CH_2Cl_2$)/B3LYP/6-31G(d) level.



NIH-PA Author Manuscript NIH-PA Author Manuscript NIH-PA Author Manuscript

NIH-PA Author Manuscript

NIH-PA Author Manuscript

NIH-PA Author Manuscript

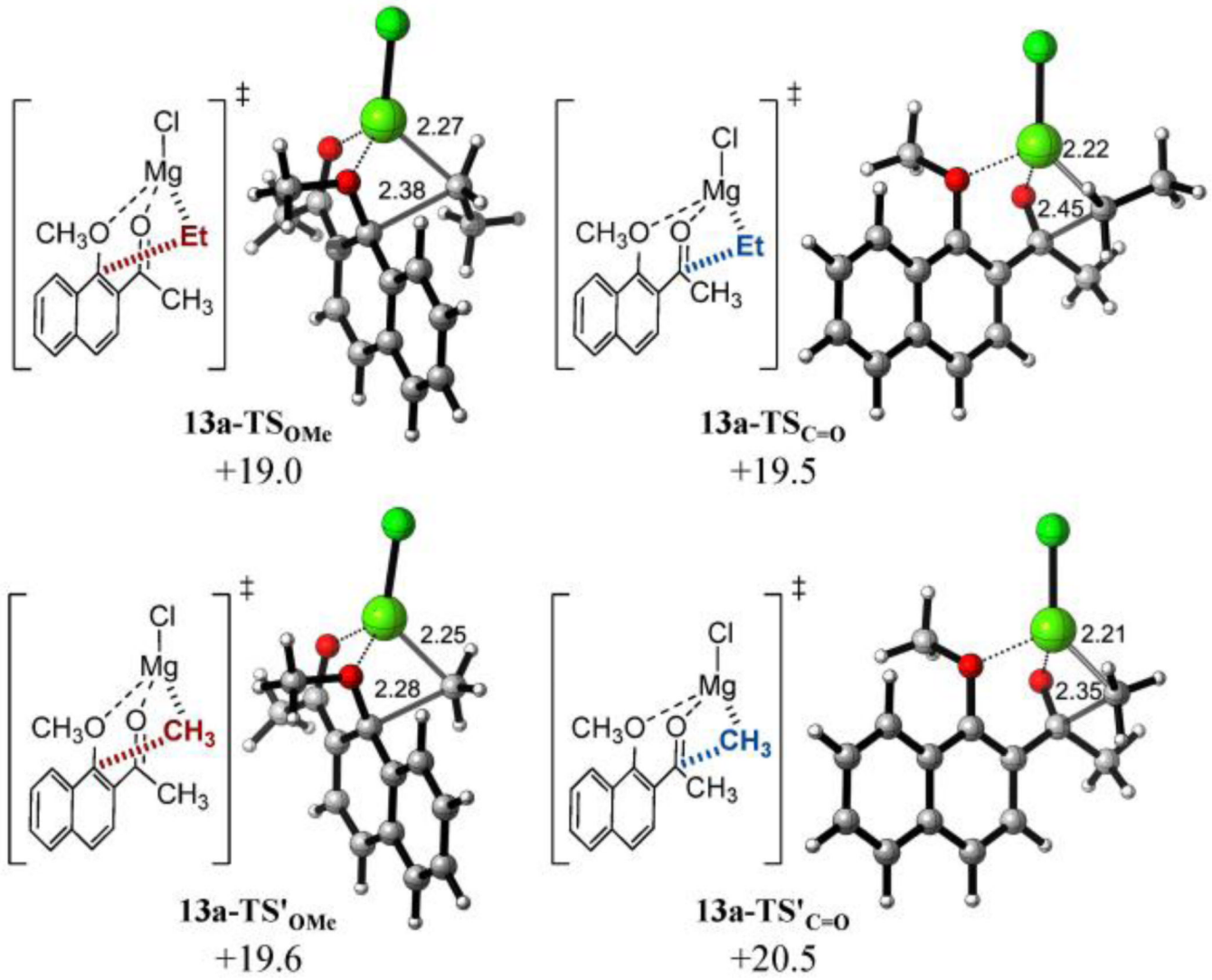


**Figure 6.**

a) Lowest-energy transition structures and activation free energies ($\Delta G^{\ddagger}$) for the reaction of nahphyl ketone **13a** with EtMgCl (top) and MeMgCl (bottom) calculated at the PCM($CH_2Cl_2$)/B3LYP/6-31G(d) level. Energies are in kcal $mol^{-1}$ and distances are in Angstrom.

NIH-PA Author Manuscript
NIH-PA Author Manuscript
NIH-PA Author Manuscript



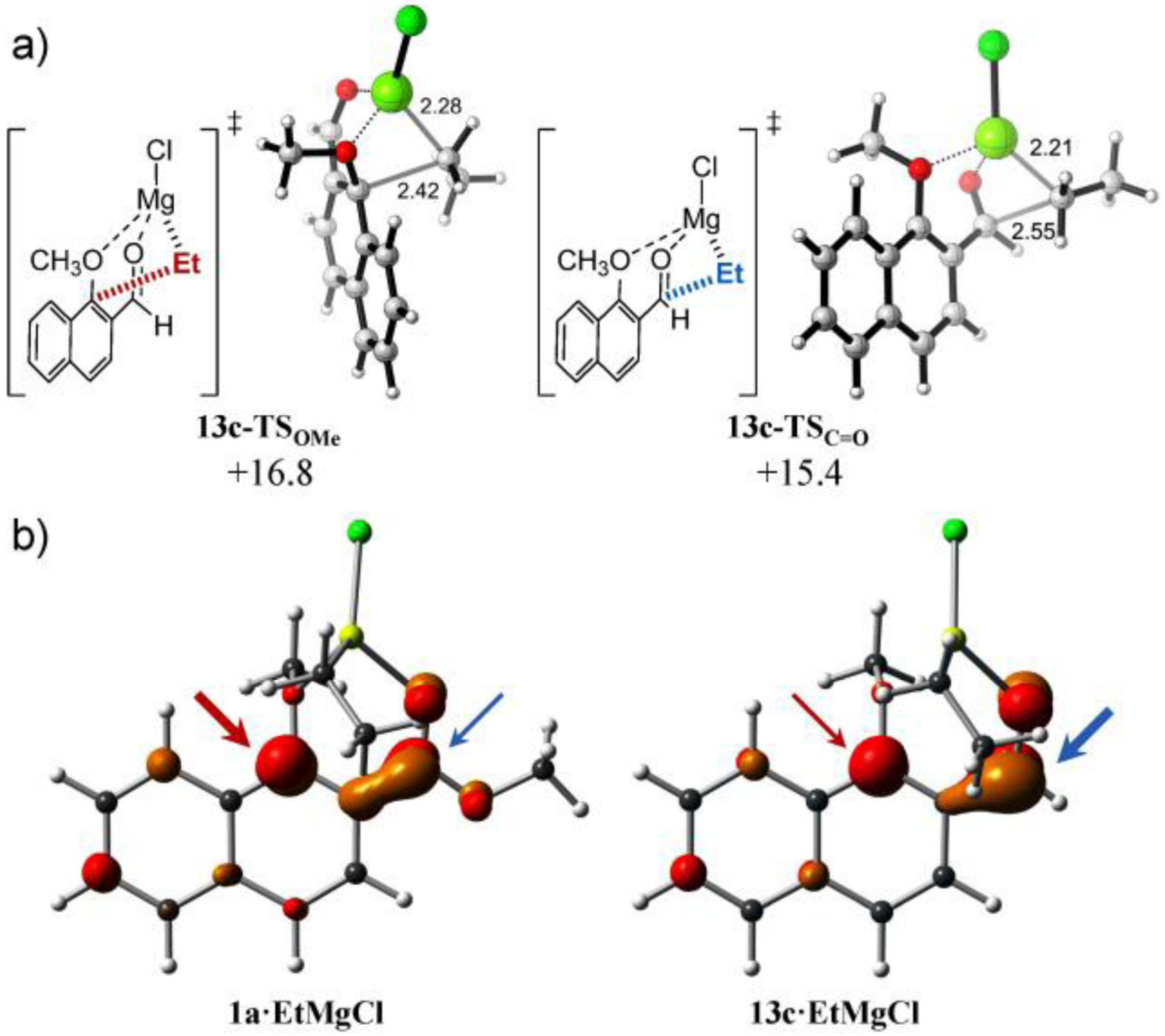


**Figure 7.**

a) Lowest-energy transition structures and activation free energies ($\Delta G^{\ddagger}$) for the reaction of nahphyl aldehyde **13c** and EtMgCl calculated at the PCM($CH_2Cl_2$)/B3LYP/6-31G(d) level. Energies are in kcal $mol^{-1}$ and distances are in Angstrom. b) Isosurface representation of LUMO of reactant complex derived from ester **1a** and aldehyde **13c**. Potentially reactive positions are marked with red (methoxy group) and blue (carbonyl group) arrows.

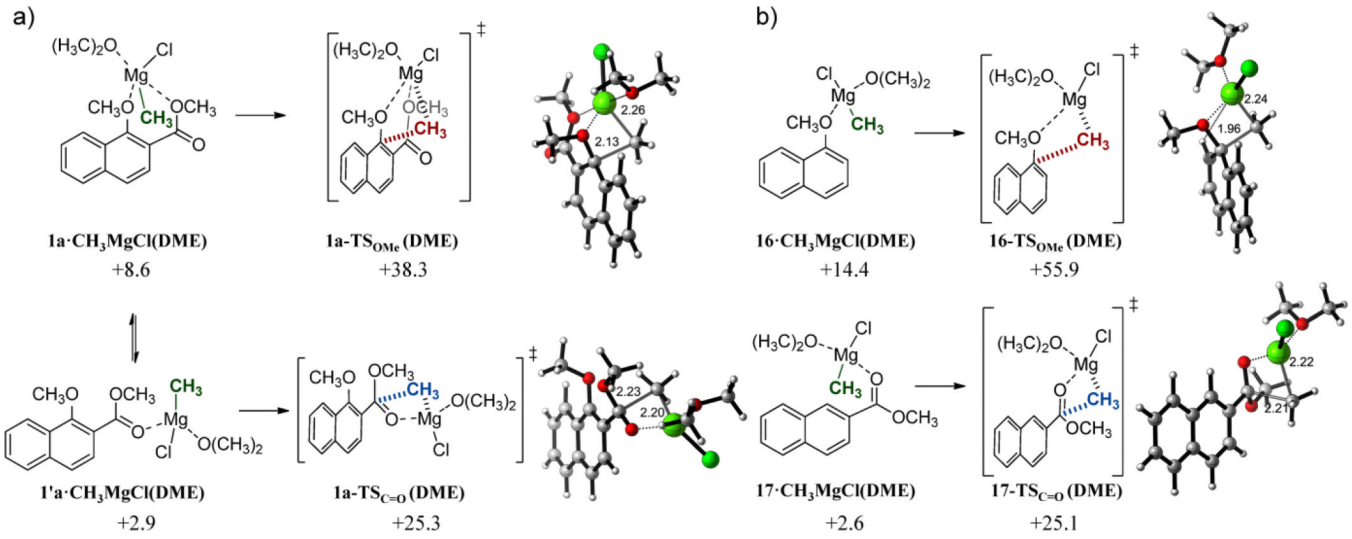


**Figure 8.**

a) Lowest-energy reactant complexes and transition structures for the reaction of nahphyl ester **1a** and **$CH_3MgCl(DME)$**. b) Lowest-energy reactant complexes and transition structures for the reaction of 1-methoxynaphthalene **16** and methyl 2-naphthoate **17** with **$CH_3MgCl(DME)$**. Complexation ($\Delta G$) and activation free energies ($\Delta G^{\ddagger}$) were calculated at the PCM($CH_2Cl_2$)/B3LYP/6-31G(d) level and are related to the isolated reactants. Energies are in kcal $mol^{-1}$ and distances are in Angstrom.



NIH-PA Author Manuscript NIH-PA Author Manuscript NIH-PA Author Manuscript

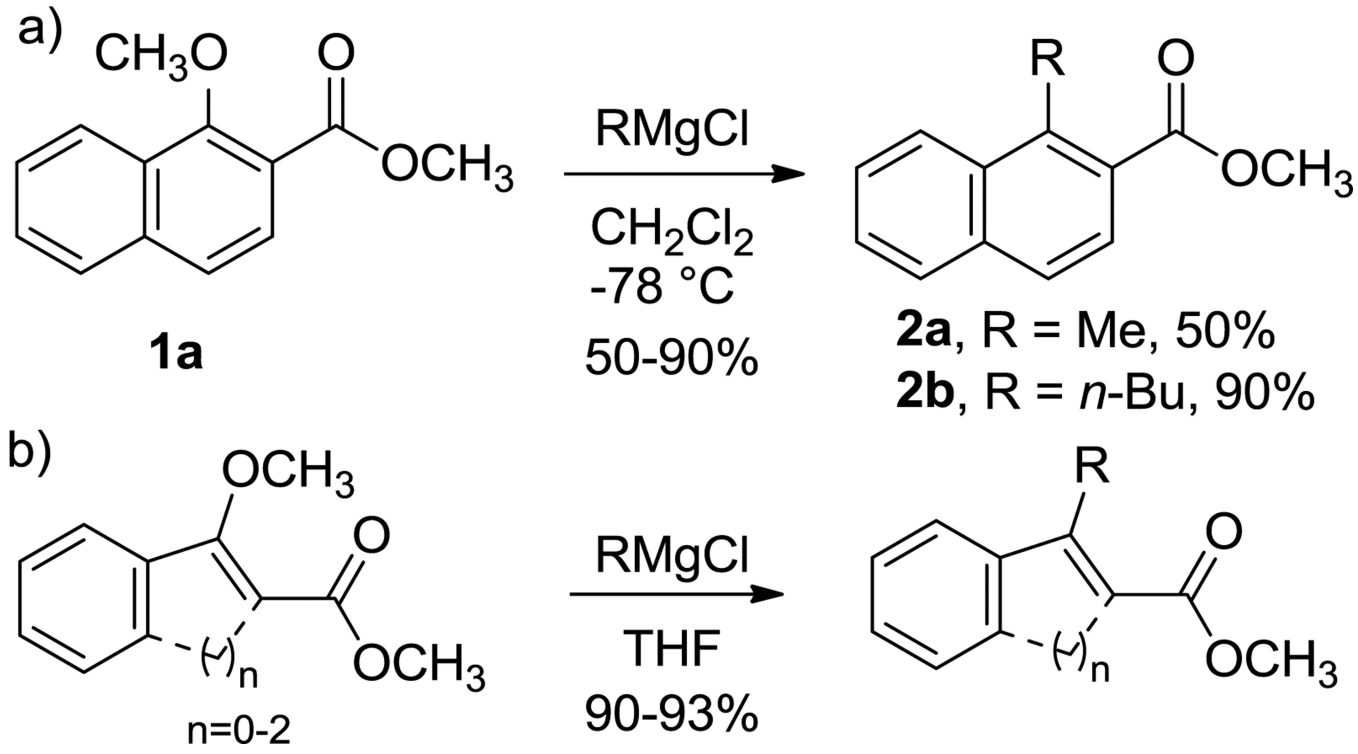


**Scheme 1.**
Displacement of alkoxy groups by Grignard reagents in aromatic (a) and non-aromatic (b) substrates.



NIH-PA Author Manuscript NIH-PA Author Manuscript NIH-PA Author Manuscript

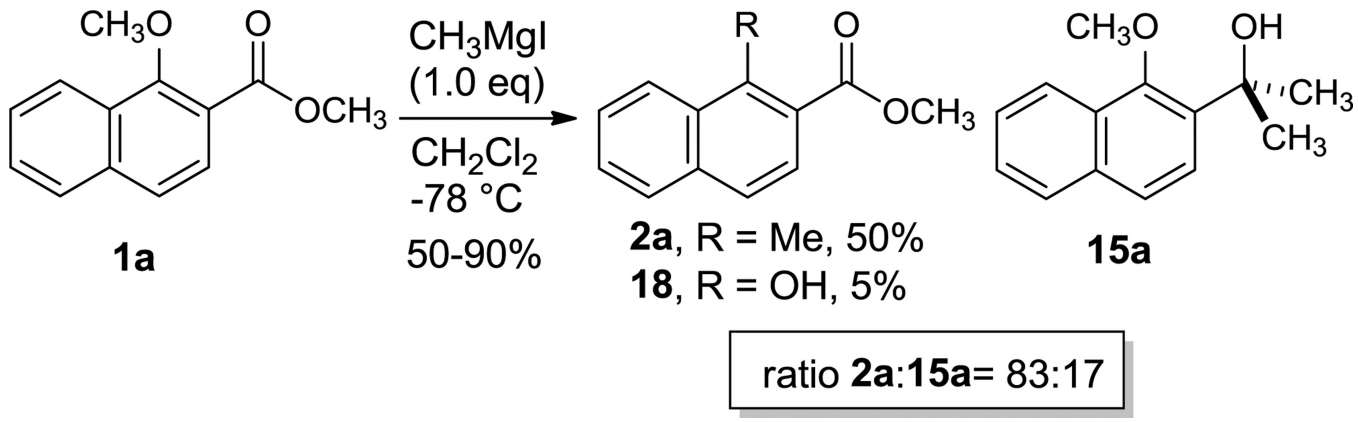


**Scheme 2.**
Reaction of aromatic β-alkoxy esters with methyl Grignard reagents.

NIH-PA Author Manuscript
NIH-PA Author Manuscript
NIH-PA Author Manuscript

NIH-PA Author Manuscript

NIH-PA Author Manuscript

NIH-PA Author Manuscript

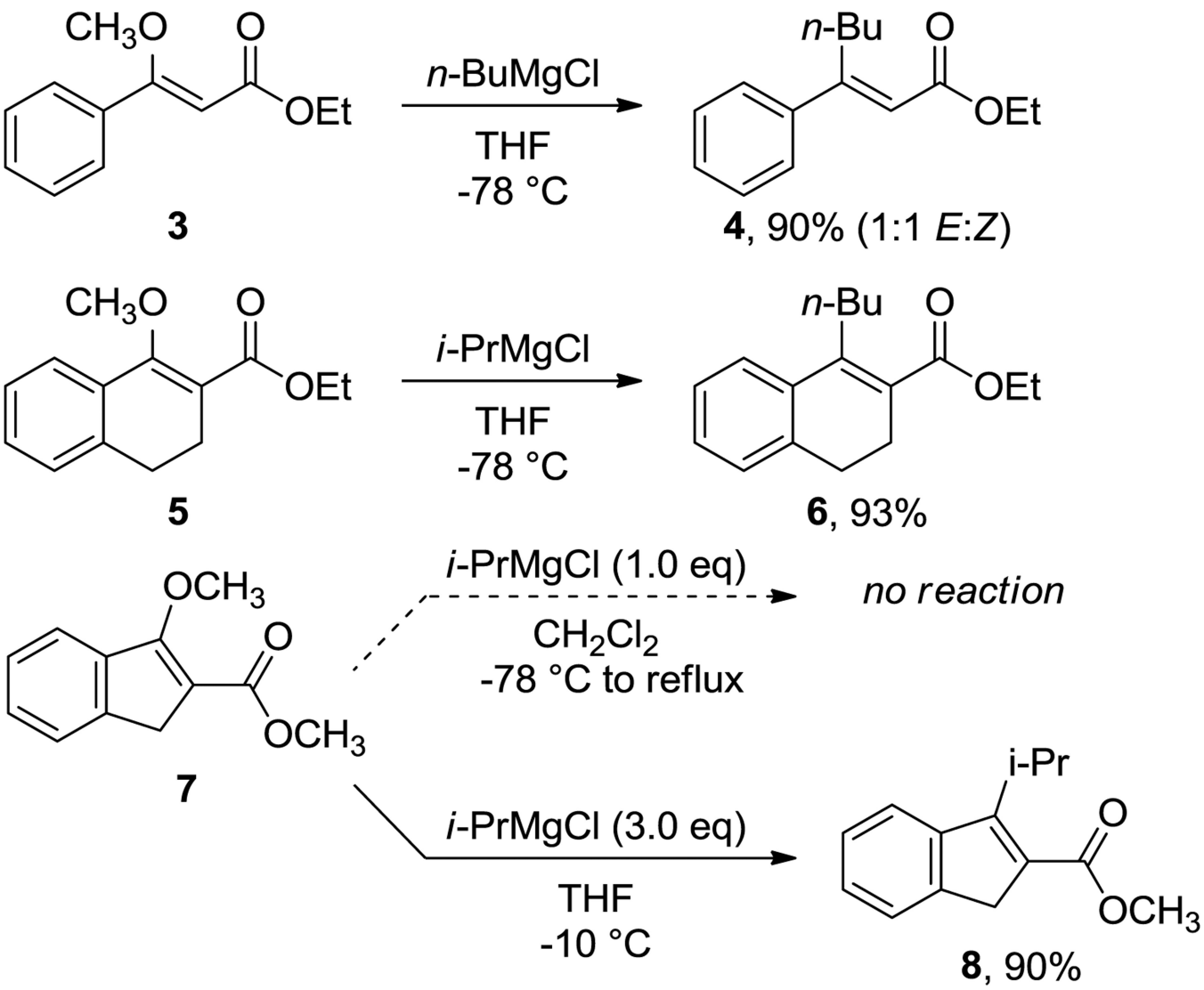


**Scheme 3.**
Reactivity of non-aromatic vinylogous esters with Grignard reagents.

NIH-PA Author Manuscript

NIH-PA Author Manuscript

NIH-PA Author Manuscript

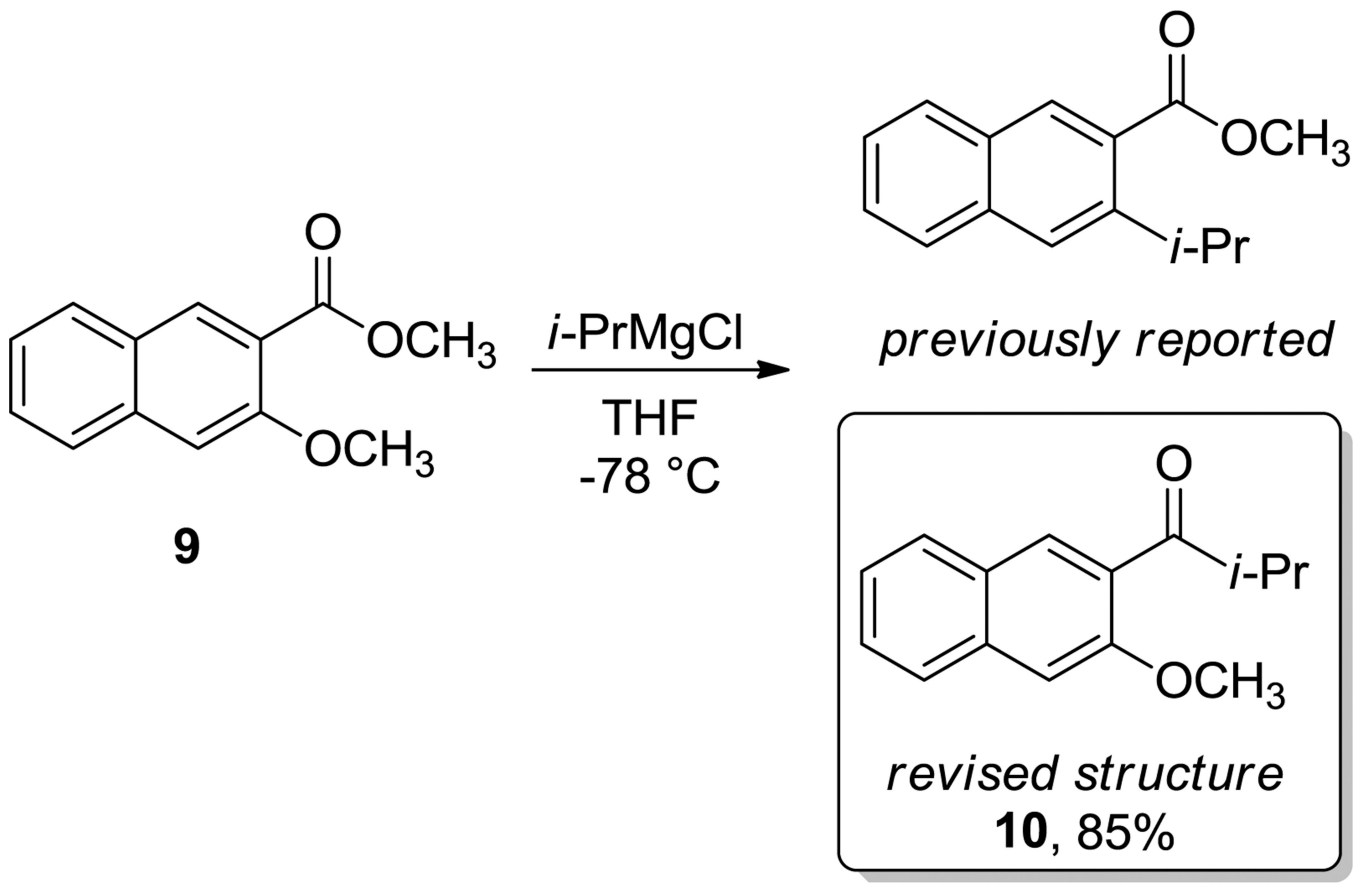


**Scheme 4.**
Structural revision of the reaction product between of naphthyl ester 9 and Grignard reagents. As predicted computationally, 1,2-addition to the carbonyl group takes place exclusively.

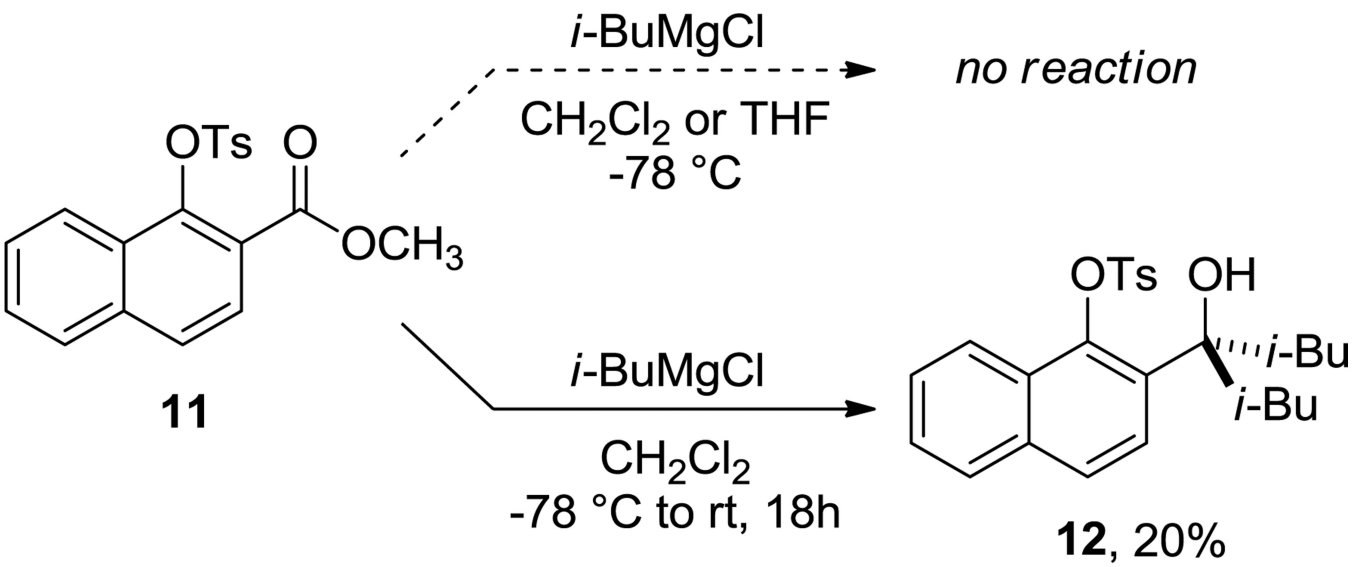


**Scheme 5.**
Reactivity of (tosyl)naphthyl esters with Grignard reagents.

NIH-PA Author Manuscript
NIH-PA Author Manuscript
NIH-PA Author Manuscript

NIH-PA Author Manuscript NIH-PA Author Manuscript NIH-PA Author Manuscript



**Table 1**

Comparison of carbonyl reactivity toward alkoxide displacement.

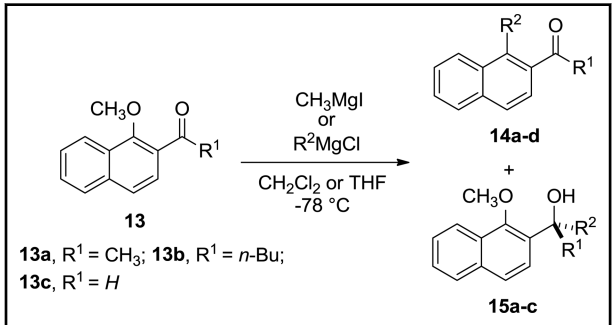


**13a**, $R^1 = CH_3$; **13b**, $R^1 = n$-Bu; **13c**, $R^1 = H$

| Entry | Substrate (R1) | R2 | Ratio of 14 : 15 | | Isolated yield, % (product) |
|---|---|---|---|---|---|
| | | | Predict.[a] | Exp.[b] | |
| 1 | **13a** | Me | 8:91 | <5:>95 | 35 (**15a**) |
| 2 | **13a** | *n*-Bu | 77:23 | 73:27 | 66 (**14a**) |
| 3 | **13a** | *i*-Pr | – | >95:<5 | 61 (**14c**) [c] |
| 4 | **13b** | *n*-Bu | 95:5 | >95:<5 | 85 (**14b**) |
| 5 | **13b** | *i*-Pr | – | >95:<5 | 90 (**14d**) |
| 6 | **13c** | *n*-Bu | 3:97 | <5:>95 | 85 (**15c**) |

[a] Calculated through a Maxwell–Boltzmann distribution at −78 °C of all computed TS.

[b] Determined by $^1$H NMR in the reaction mixture.

[c] The corresponding secondary alcohol, resulting from carbonyl reduction, was isolated in 20% yield.

*J Am Chem Soc*. Author manuscript; available in PMC 2014 May 01.